FINITE FRACTURE MECHANICS OF MATRIX MICROCRACKING IN COMPOSITES

JOHN A. NAIRN

INTRODUCTION

The first form of damage in composite laminates is often matrix microcracks that are defined as intralaminar or ply cracks across the thickness of the ply and parallel to the fibers in that ply (see reviews in [1,2]). Tensile loading, fatigue loading, environment, and thermal cycling can all lead to microcrack formation. Microcracks can form in any ply that has a significant component of the applied load transverse to the fibers in that ply. Microcracks lead to degradation in properties of the laminate including changes in effective moduli, Poisson ratios, and thermal expansion coefficients [3]. Although these changes are sometimes small, microcracks can nucleate other forms of damage. For examples, microcracks can lead to delaminations, cause fiber breaks, and provide pathways for entry of corrosive liquids. An important issue in design of composite laminates is to be able to predict the initiation and development of microcracking damage following complex loading conditions. This chapter describes a fracture mechanics approach to the microcracking problem.

A complicating feature of composite fracture mechanics analysis is that laminates often fail by a series of fracture events instead of by continuous crack growth. Microcracking is a prime example. When cross-ply laminates are loaded in tension, the microcracking process is a series of events in which a single microcrack forms and instantaneously (on observation time scale) propagates until it fills the entire cross-sectional area of the ply. Conventional fracture mechanics deals with predicting the propagation of an existing crack. One could imagine analyzing microcrack propagation within a ply by standard methods, but there is little incentive to tackle this problem. The analysis could not be compared to experimental results for events and the analysis of a single crack does not answer the problem of predicting the extent or number of microcracks that form under various loading histories. Some microcracking models have abandoned fracture mechanics and used critical stress criteria instead; these models do not work well [4]. A better approach is to extend fracture mechanics methods to handle fracture events. Hashin has coined the term “finite fracture mechanics” to describe prediction of fracture events by comparing the total energy released due to a finite amount of crack area to an event toughness [5]. A finite fracture mechanics model for matrix microcracking can correlate a

large body of experimental observations and can predict the extent of microcracking damage under various loading conditions [1,2].

FINTE FRACTURE MECHANICS PRINCIPLES

The development of a finite amount of fracture area, ΔA, must conserve energy. By the first law of thermodynamics, energy balance for an elastic material can be expressed as

$$\frac{\Delta w}{\Delta A} - \frac{\Delta U}{\Delta A} = 2\gamma + \frac{\Delta K}{\Delta A} \tag{1}$$

where w is external work, U is internal energy, γ is surface energy, and K is kinetic energy. Conventional fracture mechanics deals with infinitesimal static crack growth for which $\Delta A \to da$ and $\Delta K \to 0$. Crack growth occurs when energy release rate, G, is equal to the critical energy release rate, G_c:

$$G = \frac{dw}{dA} - \frac{dU}{dA} = 2\gamma = G_c \tag{2}$$

G_c is used in place of 2γ because experimental observations show that energy released during crack growth is always much larger than the thermodynamic surface energy (2γ). In other words, G_c is an *effective* material property that accounts for crack-tip energy dissipation not included in a linear-elastic stress analysis of crack-tip stresses. The logical extension to finite fracture mechanics is to assume a fracture event occurs when

$$G^* = \frac{\Delta w}{\Delta A} - \frac{\Delta U}{\Delta A} = 2\gamma + \frac{\Delta K}{\Delta A} = G_c^* \tag{3}$$

Here G^* is a finite energy release rate and G_c^* is an *effective* material property or event toughness that accounts for energy dissipation and kinetic energy effects not included in static linear-elastic analysis of work and energy before and after a fracture event. Conventional fracture mechanics works well provided G_c is found to be independent of specimen geometry. Similarly, finite fracture mechanics works well provided G_c^* is independent of specimen geometry and current damage state and provided initiation of the event is facilitated by conditions such as existing flaws or stress concentrations. The appearance of ΔK in G_c^* might render some fracture events unsuitable for finite fracture mechanics. ΔK can be included in an *effective* toughness, however, provided either it is small ($\Delta K << G^*$) or it is a constant that is characteristic of a particular fracture event [6].

APPLICATION TO MICROCRACKING

To verify the use of finite-fracture mechanics for microcracking, predictions can be compared to experiments. The procedure is to evaluate G^* and then predict microcrack formation by assuming the next crack forms when $G^* = G_c^*$. A unique feature of finite fracture mechanics is that G^* is different for load-control *vs*. displacement-control experiments [2,6]. Most static experiments use displacement control, but fatigue or thermal cycling experiments use load control. Both conditions must be analyzed. By using global energy methods, which include residual stresses effects [7], G^* for formation of a new microcrack in a $[0_n/90_m]_s$ laminate

midway between two existing microcracks separated by $2mt_{ply}\alpha_i$, where t_{ply} is thickness of a single ply, can be expressed exactly as [2]

$$G^* = \frac{\sigma_{90}^2 \alpha_i B}{2k_m^2}\left[\frac{1}{E_A(\alpha_i/2)} - \frac{1}{E_A(\alpha_i)}\right] \quad \text{(load control)} \tag{4}$$

$$G^* = \frac{E_{A,N}^* E_{A,N+1}^*}{E_{A,0}^{*\,2}} \frac{\sigma_{90}^2 \alpha_i B}{2k_m^2}\left[\frac{1}{E_A(\alpha_i/2)} - \frac{1}{E_A(\alpha_i)}\right] \quad \text{(displacement control)} \tag{5}$$

Here $\sigma_{90} = k_m\sigma_{app} + k_{th}\Delta T$ is the stress transverse to the fibers in the 90° plies in the absence of damage (it is linearly related to applied load, σ_{app}, and temperature difference, ΔT, by laminate-dependent mechanical and thermal stiffnesses, k_m and k_{th}), B is laminate thickness, and $E_A(\alpha)$ is the effective axial modulus of a microcracking interval of dimensionless length α. In the displacement-control equation, $E_{A,N}^*$ is the axial modulus of a damaged laminate with N microcracks. Analogous, but different, results can be derived for microcracking of surface plies in $[90_m/0_n]_s$ laminates [2].

Figure 1 compares predictions to experiments for three different cross-ply laminates. All results are fit well with $G_c^* = 230 \pm 30$ J/m^2. The analysis for these experiments required input of $E_A(\alpha)$ and α_i. $E_A(\alpha)$ can be found by various stress-analysis methods [1]. The analysis for Fig. 1 used a complementary energy solution [8]. Simpler, albeit less accurate, shear lag methods are available [9]. The complementary energy solution loses accuracy when the ratio of the 0° to 90° thicknesses increases [10]; for these geometries $E_A(\alpha)$ can be found by potential energy solutions or by numerical methods [2,10]. The term α_i is the dimensionless length of the microcracking interval where the next crack forms. This term is not the *average* crack spacing because experimental observations and theory both reveal that larger crack intervals are more likely to crack than smaller crack intervals. Unless experiments are coupled with direct observation of each microcracking event, the recommended analysis method is to replace α_i by $f\langle\alpha\rangle$ where f is a parameter greater than 1 and $\langle\alpha\rangle$ is the average microcrack spacing [2,4]. In a deterministic microcracking model where the crack always forms in the largest crack interval, f would oscillate between 1 and 2 or average 1.5. Alternately f can be measured by monitoring the microcracking process [11] or by adjusting it to fit experimental results [4]. Both these approaches show f to be between 1.2 and 1.5.

The advantage of finite fracture mechanics analysis of microcracking is that a single material property, G_c^*, can correlate data for different layups, such as the three layups in Fig. 1. To verify this important fracture mechanics result for more experiments, the microcrack formation criteria can be cast in a master plot form [4] by rewriting Eqs. (4) and (5) (and analogous expressions for laminates with surface 90° plies) as

$$\sigma_{red} = D_{red}\sqrt{G_c^*} + \Delta T \tag{6}$$

where σ_{red} and D_{red} are reduced stress and crack density defined by

$$\sigma_{red} = \left(\frac{k_m}{k_{th}}\right)\sigma_{app} \quad \text{and} \quad D_{red} = \left(\frac{1}{k_{th}\sqrt{G_{unit}^*}}\right) \tag{7}$$

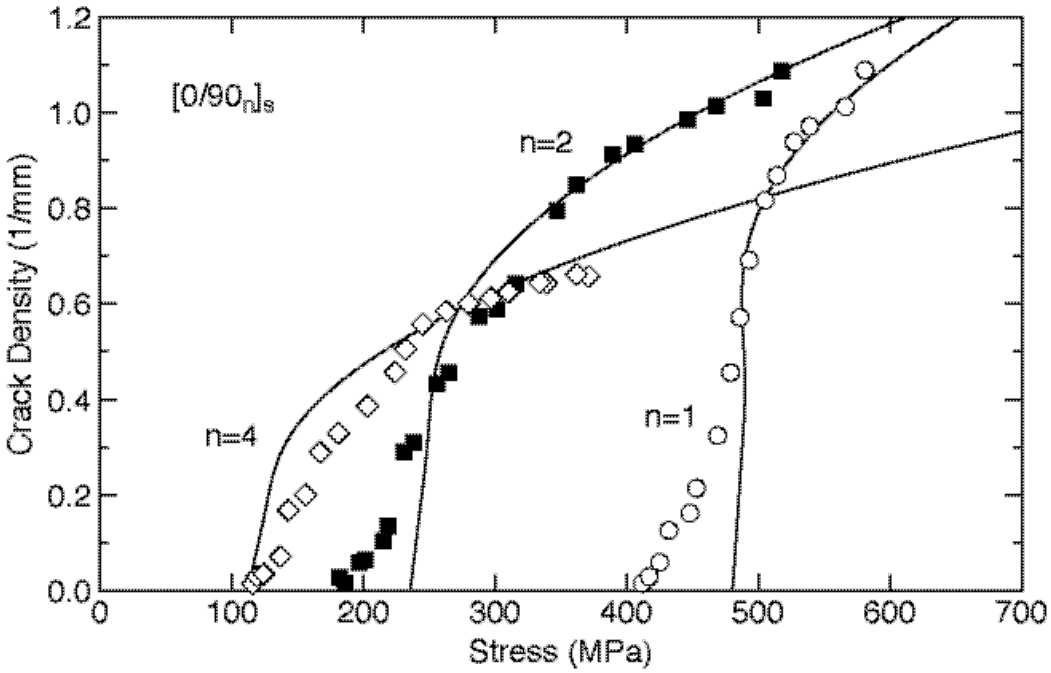

Fig. 1. Microcrack density as a function of applied stress for three Hercules AS4/3501-6 cross-ply laminates. The smooth lines are finites to finite fracture mechanics theory assuming G_c = 230±30 J/m^2 and $\Delta T = -100^\circ C$.

Here G^*_{unit} is the normalized energy release rate for unit Δ_{90}. If finite fracture mechanics works well, a plot of Δ_{red} as a function of D_{red} should be a straight line. The slope of the line gives the microcracking toughness and the intercept gives the thermal stress term. A sample master plot is given in Fig. 2 [4]. The results from 14 different layups, including both central (open symbols) and surface (filled symbols) cracked plies, all fall on the same line.

DISCUSSION

In typical microcracking experiments, microcracks form as a series of events. Experimental results consist of recording the number of microcracks as a function of loading conditions and specimen geometry. More detailed information could include the distribution of microcracking spacings [11]. If microcracks form in multiple ply groups (such as cracks on each surface of $[90_n/0_m]_s$ laminates), it is important to record correlations between damage states of the various plies. For transparent composites, full microcracks can be observed. For opaque composites, microcracks can be observed only on the edge. It is important to verify such microcracks correspond to a complete microcrack by observing opposite edges or by using x-ray methods. Microcracking experiments have been done by static tensile loading [1,2], mechanical fatigue [12], thermal cycling fatigue [13], and environmental exposure [14]. Static results are best analyzed by the methods above. Fatigue and thermocycling results can be analyzed by a modified Paris law where the rate of increase in crack density, D, per cycle, N, is related to the range in energy release rate, ΔG^*, by

$$\frac{dD}{dN} = K\left(\Delta G^*\right)^m \tag{8}$$

where K and m are fatigue toughness properties.

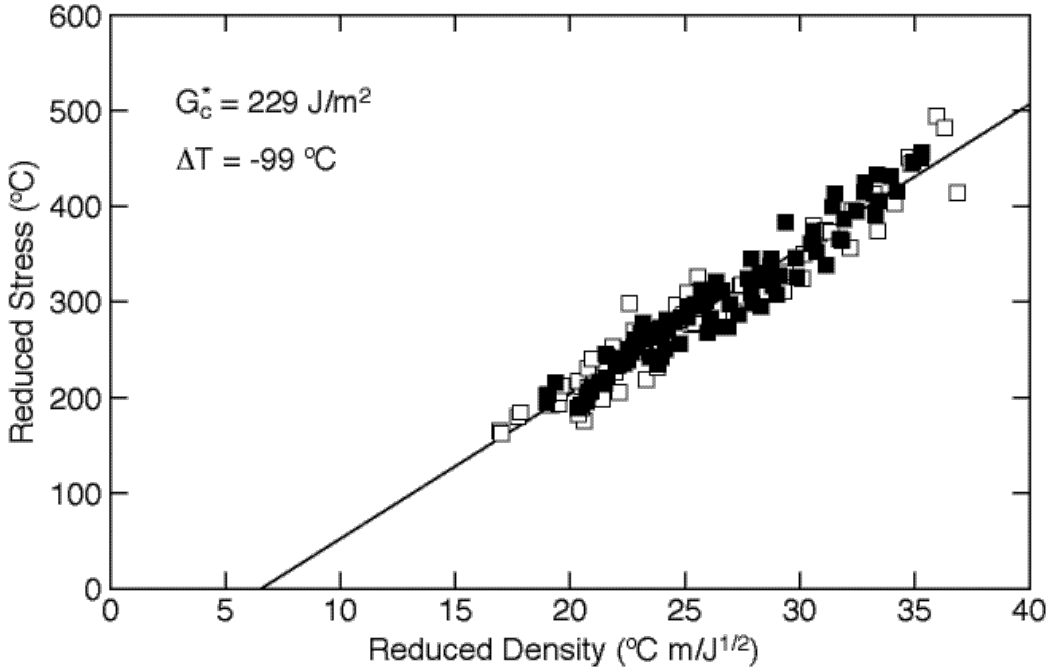

Fig. 2: Master plot results for 14 different layups of Hercules AS4/3501-6 laminates. The open symbols are for $[0_m/90_n]_s$ laminates; the filled symbols are for $[90_n/0_m]_s$ laminates. The straight line is a fit to all results; the slope and intercept give $G_c = 229$ J/m^2 and $\Delta T = -99$°C.

The master plot in Fig. 2 shows that finite fracture mechanics of microcracking captures all major features of the microcracking process. There are minor details, however, and systematic effects that require further analysis. For example, the onset and initial rise in crack density is typically slower in experiments than as predicted by theory (see Fig. 1). This effect can be explained by introducing statistical variations in G_c^*. The early microcracks occur where the toughness is low; the later cracks are controlled by geometry (*i.e.*, they form midway between existing microcracks). Statistical variations can be included in the analysis by using simulations to fit experiments [2]. The results of such fits are that the mean toughness is similar to the toughness calculated by the simpler methods. The early crack density data gives new information about material variability. Simulations naturally account for the effect of microcracks to occur in larger microcracking intervals and thus do not need an f factor. Simulations results show that f is between 1.3 and 1.5 [11].

When G_c^* is found by fitting to individual layups, rather than a global master plot, there is a systematic trend towards lower toughness as the strain to initiate microcracking increases. This trend suggests that loading is causing diffuse damage in the microcracking plies that is causing a drop in G_c^*. Laminates that initiate microcracks at low strain (*e.g.*, laminates with thick 90° plies) have less damage and thus have a higher *apparent* toughness. Laminates that initiate at higher strain show a slightly lower toughness. This effect can be analyzed by continuum damage mechanics methods [10]. By using numerical methods and plotting G^* as a function of dimensionless crack spacing, $\Box$, it was observed that G^* is a property of the ply material but independent of the supporting plies. This observation made it possible to incorporate finite fracture mechanics methods into continuum damage mechanics models. By coupling a diffuse damage evolution law with microcracking toughness, a wider range of laminate structures can be predicted with greater accuracy [10].

REFERENCES

1. J. A. Nairn and S. Hu (1994) in *Damage Mechanics of Composite Materials*, eds., Ramesh Talreja, Elsevier Science, The Netherlands, 187-243.
2. J. A. Nairn (2000) in *Polymer Matrix Composites*, eds., R. Talreja and J.-Å. E. Manson, Elsevier Science, The Netherlands, 403-432.
3. L. N. McCartney (2000) *Comp. Sci. & Tech.* **60**, 2255-2279.
4. J. A. Nairn, S. Hu, and J. S. Bark (1993) *J. Mat. Sci.* **28**, 5099-5111.
5. Z. Hashin (1996) *J. Mech. & Phys. Solids* **44**, 1129-1145.
6. J. A. Nairn (1999) *5th Int'l Conf. on Def. and Fract. of Composites*, London, UK, March 18-19.
7. J. A. Nairn (2000) *Int. J. Fract.* **105**, 243-271.
8. Z. Hashin (1985) *Mech. of Mater.* **4**, 121-136.
9. K. W. Garrett and J. E. Bailey (1977) *J. Mat. Sci.* **12**, 157-168.
10. P. Ladevèze and G. Lubineau (2001) *Comp. Sci. & Tech.* **61**, 2149-2158.
11. D. Bal (2001) *M.S. Thesis*, MS&E Dept., University of Utah.
12. L. Boniface and S. L. Ogin (1989) *J. Comp. Mat.* **23**, 735-754.
13. C. Henaff-Gardin, M. C. Lafarie-Frenot, and J. L. Desmeuzes (1995) *Proc. ICCM-10*, Vancouver, BC, Canada, Aug 14-18.
14. M. H. Han and J. A. Nairn (2002) *Composites, Part A*, submitted.